Ferroelectric and dielectric properties of $Bi_{3.15}Nd_{0.85}Ti_3O_{12}$ nanotubes

Wei Cai,[1,2] Xiaomei Lu,[1,a)] Huifeng Bo,[1] Yi Kan,[1,b)] Yuyan Weng,[1] Liang Zhang,[1] Xiaobo Wu,[1] Fengzhen Huang,[1] Lukas M. Eng,[3] Jinsong Zhu,[1] and Feng Yan[4,c)]
[1]*National Laboratory of Solid State Microstructures, School of Physics, Nanjing University, Nanjing 210093, People's Republic of China*
[2]*School of Physics, Guangzhou University, Guangzhou 510006, People's Republic of China*
[3]*Institut für Angewandte Photophysik, Technische Universität Dresden, D-01062 Dresden, Germany*
[4]*Department of Applied Physics, Hong Kong Polytechnic University, Kowloon, Hong Kong, People's Republic of China*

(Received 22 December 2010; accepted 13 June 2011; published online 2 September 2011)

In order to match the high-density requirement of ferroelectric memories, ferroelectric $Bi_{3.15}Nd_{0.85}Ti_3O_{12}$ nanotubes with outer diameter of about 100 nm and wall thickness of about 30 nm were synthesized using a sol-gel method. Transmission electron microscope images and Raman spectra revealed the Bi-layered perovskite structure of these nanotubes. Their dielectric constant and remnant polarization were comparable with those of thin film form. Piezoelectric hysteresis loops of individual nanotube measured by piezoresponse force microscope indicate their asymmetry, and the switched nanotubes show long term retention. © *2011 American Institute of Physics*. [doi:10.1063/1.3624801]

I. INTRODUCTION

Ferroelectrics have attracted much attention for their applications in nonvolatile memories, microelectromechanical systems, and nonlinear optics.[1–4] In recent research on ferroelectrics, piezoresponse force microscopy (PFM) plays a more and more important role.[5–7] With the help of PFM, research of ferroelectricity extends to nanometer scale,[8–12] which is direct and effective to understand the frequently reported size effect of ferroelectricity and in turn the miniaturization of devices.[13–15] In these decades, ferroelectric nanotubes have been paid much attention because of their multi-dielectric-surface of the tubular structure. Based on the characteristic of three-dimensional (3D) tubular stacking, the miniaturization of ferroelectric random access memories (FeRAMs) can be greatly improved.

Differing from bulk and thin film forms, ferroelectric nanotubes exhibit many novel properties. It is reported that the $PbZr_{0.52}Ti_{0.48}O_3$ (PZT) nanotube arrays can provide THz emission.[16] The periodic boundary condition can lead to a surface tension, which improves the polarization of PZT nanotubes.[17] To date, numerous perovskite ferroelectric nanotubes have been synthesized and characterized, such as PZT, $BaTiO_3$, $BiFeO_3$, and so on.[18–22] However, few works have been done on Bi-layered perovskite ferroelectric nanotubes, which are lead free, fatigue free, and possess larger and more anisotropic crystalline cells compared to those of simple perovskites. Although $SrBi_2Ta_2O_9$ (Ref. 23) and doped-$Bi_4Ti_3O_{12}$ (Refs. 24 and 25) nanotubes have been successfully fabricated, further studies are still needed to explore their basic physical properties.

In our previous work,[26] $Bi_{3.15}Nd_{0.85}Ti_3O_{12}$ (BNT) nanotubes have been synthesized and their optical-transmittance measurements show a special shift of the energy gap related to the 3D tubular structure. In this paper, we focus on the electrical properties of BNT nanotubes, especially their ferroelectric and dielectric properties.

II. EXPERIMENTAL PROCEDURE

Polycrystalline BNT nanotubes were fabricated using a method described as follows:

(1) Bismuth nitrate, neodymium oxide, and tetra-butyl titanate were used to provide Bi, Nd, and Ti, respectively, and acetic acid was used as solvent. The concentration of the precursor solution was diluted to 0.2 mol/L by adding 2-methoxyethanol.
(2) High purity (99.999%) aluminum foils were first baked at 500 °C, and then anodization was carried out for 10 h under a dc voltage of 50 V in oxalic acid (0.3 mol/L) with ambient temperature of 30 °C. After that, saturated $CuCl_2$ solution was used to remove the remnant aluminum. The pore ends were opened and enlarged by 6 wt. % H_3PO_4 at room temperature for obtaining the desired anodic aluminum oxide (AAO) templates.
(3) For fabricating BNT nanotube arrays, the AAO templates were immersed into the BNT precursor solution for 12 h to make a complete infiltration. Thereafter, the AAO templates containing the precursor solution were heated up to 700 °C within 2.5 h in oxygen atmosphere followed by an annealing of 0.5 h. The outer diameters, wall thicknesses, and lengths of individual BNT nanotubes were about 100 nm, 30 nm, and 50 μm, respectively.

For the measurement of dielectric and ferroelectric properties using RT66A, the BNT nanotubes with AAO templates were double-side polished until their length was on

a)Author to whom correspondence should be addressed: Electronic mail: xiaomeil@nju.edu.cn.
b)Electronic mail: yikannju@gmail.com.
c)Electronic mail: apafyan@inet.polyu.edu.hk.

the order of 1 μm, and Pt was deposited as the testing electrode. For Raman spectra and PFM study, the AAO templates containing BNT nanotubes were etched by NaOH solution (2 mol/L), and then washed by de-ionized water to remove the remnant alkaline solute. The fabricated BNT nanotubes were dissolved and dispersed in ethanol, and finally deposited onto $Pt/Ti/SiO_2/Si$ substrates. The Raman spectrum were acquired on a T64000 triple Raman system with backscattering geometries using the 514.5 nm line of an Ar^+ laser as excitation source. The PFM study was realized on the basis of a commercial Explorer^{TM} Scanning Probe Microscope and two lock-in amplifiers (SR830, Stanford Research Systems). An ac modulation voltage with frequency of 18 kHz and amplitude of 1.5 V was applied between the conductive tip (Cr/Pt coated Si with resonance frequency of 75 kHz) and the bottom Pt electrode for piezoresponse measurement.

III. RESULTS AND DISCUSSIONS

Figure 1(a) gives the transmission electron microscope (TEM) image of an individual BNT nanotube with outer diameter around 100 nm. A high resolution TEM (HRTEM; TF-20, FEI) image of a BNT nanotube [Fig. 1(b)] indicates that the lattice spacings are 0.271 nm and 0.272 nm, which correspond to the (020) and (200) planes, respectively. The (115) and (208)/(028) planes can also be identified by the lattice spacings of 0.332 nm and 0.263 nm as shown in Figs. 1(c) and 1(d).

It is known that tetragonal BNT belongs to the I4/mmm space group and there are 16 Raman-active modes ($6\ A_{1g} + 2B_{1g} + 8E_g$).[27] Fig. 2 gives the Raman spectrum of an individual BNT nanotube, inset of which is the image obtained by scanning electron microscope. There are four distinguishable Raman peaks in Fig. 2. The Raman shift peak at around 60 cm^{-1} corresponds to the rigid-layer (RL) mode,[28] which originates from the movement of the layer-like rigid units of $(Bi_2O_2)^{2+}$ in Bi-layered structures. In the high wavenumber region, three major peaks located at around 277, 558, and 834 cm^{-1} can be identified as A_{1g} mode, which is attributed to the internal vibration modes of TiO_6 octahedron for its stretching and distortion.[29,30] This mode is considered to have great impacts on the ferroelectricity of BNT. The wall thickness of a BNT tubular structure is only about 30 nm, which greatly suppresses the grain size. The broken symmetry makes the Raman peaks of BNT nanotubes broaden and some of the peaks are ambiguous to identify. Compared with that of the single crystal form[27] and BNT films (852 cm^{-1}, not shown here), the Raman peak of the nanotube at around 834 cm^{-1} shifts to lower wavenumber evidently, which indicates that the increased distortion of TiO_6 octahedron is possibly related with the larger internal stress.[30] The stress induced distortion[22,30] is considered to potentially enhance the polarization of ferroelectric nanotubes.

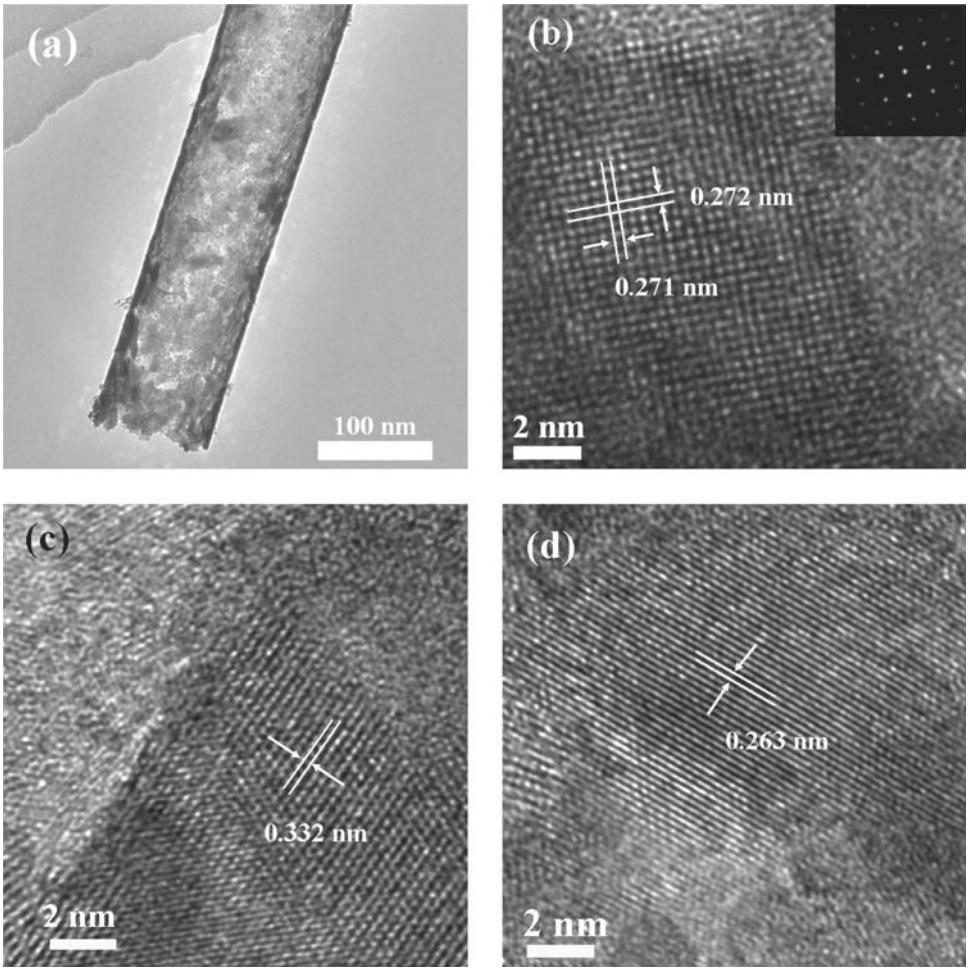

FIG. 1. (a) TEM and (b)–(d) HRTEM images of BNT nanotubes. The inset of Fig. 1(b) shows the FFT of corresponding area.

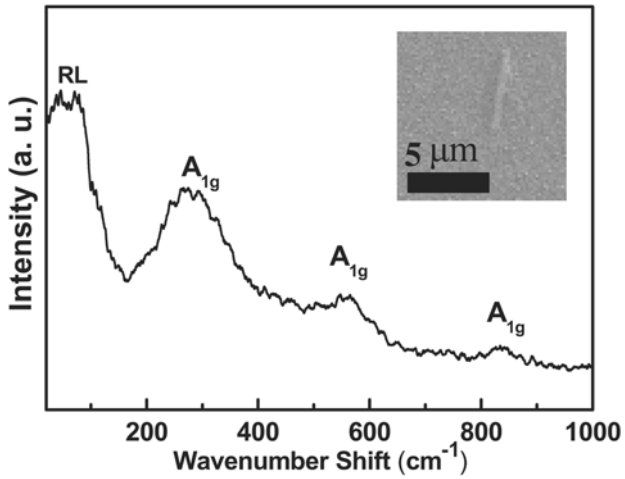

FIG. 2. Raman spectrum of a single BNT nanotube measured at room temperature. The inset shows the single BNT nanotube in the scope area of micro-Raman measurement.

The BNT nanotubes embedded in the AAO templates can be considered as parallel-connected capacitors of BNT nanotubes and alumina. The dielectric constant (ϵ) of BNT nanotubes can be calculated by $C = C_{BNT} + C_{AAO}$, where C, C_{BNT}, and C_{AAO} are the capacitances of BNT and AAO composites, BNT nanotubes, and AAO templates, respectively. The dielectric constants and losses of BNT nanotubes and AAO templates as a function of frequency are shown in Fig. 3. The inset gives the dielectric constant and loss ($\tan\delta$) of blank AAO templates. It is found that the dielectric constant of blank AAO templates is of about 4.5 at 10^6 Hz, and it increases to about 7.5 when the template is filled by BNT nanotubes. The calculated dielectric constant of pure BNT nanotubes is of about 200 at 10^6 Hz, which is comparable to that of BNT thin films.[31] The decrease of ϵ with the increasing frequency from 500 Hz to 1 kHz denotes the dipole relaxation,[32] while the flat relationship of ϵ-f from 10^3 Hz to 10^6 Hz indicates a low concentration of defects.

Figure 4 shows the ferroelectric hysteresis loops of BNT nanotubes and AAO templates. As we know, the AAO template is not ferroelectric and do not exhibit hysteresis loops as the electric field is applied (inset of Fig. 4), although some charged particles in the surface may respond slightly. This means that the ferroelectricity measured in Fig. 4 is mainly originated from the fabricated BNT nanotubes. The remnant polarization (P_r) is of about 0.5 $\mu C/cm^2$. Estimated from SEM observation,[26] the effective contact area of the BNT nanotubes under the top electrode is only 5%. Thus, the estimated P_r of BNT nanotubes should be of about 10 $\mu C/cm^2$, which is also comparable to that of the thin film form.[31]

A PFM was employed in order to further investigate the ferroelectric properties of BNT nanotubes.[33–36,38] The out-of-plane and in-plane piezoresponse phase and amplitude loops of individual BNT nanotubes were shown in Fig. 5. There are three points we would like to mention:

(1) Both the out-of-plane [Fig. 5(a)] and in-plane [Fig. 5(c)] piezoresponse phase loops show a well-defined "square" shape, which confirms the existence of switchable domains of BNT nanotubes in both out-of-plane and in-plane directions, even though the growth of BNT grains is limited by the nanotube structure. The corresponding out-of-plane [Fig. 5(b)] and in-plane [Fig. 5(d)] piezoresponse amplitude loops show a "butterfly" shape, which implies the piezoelectric response.
(2) Both out-of-plane piezoresponse phase and amplitude show comparable intensity with those of in-plane. It is reported that, for single crystalline $BaTiO_3$ nanowires, the out-of-plane piezoresponse phase may be suppressed by the vertical size and does not show an obvious hysteresis loop.[37,39] However, our BNT nanotube shows distinguished hysteresis loop in the out-of-plane direction, which, in corresponding to the observed shift of the 834 cm^{-1} Raman peak, might be related to the increased stress in the BNT nanotube, as well as to the periodic boundary conditions.[17,30]
(3) Unlike the symmetric in-plane piezoresponse phase and amplitude loops, the out-of-plane loops show an offset. This asymmetric behavior could be attributed to the tubular structure in nanoscale and to the substrate clamping.[35]

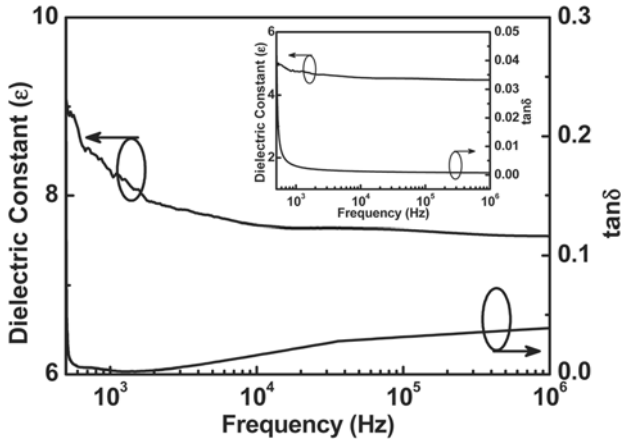

FIG. 3. Dielectric constant and loss of BNT nanotube arrays with AAO templates as a function of frequency. The inset shows the dielectric constant and loss of pure AAO templates.

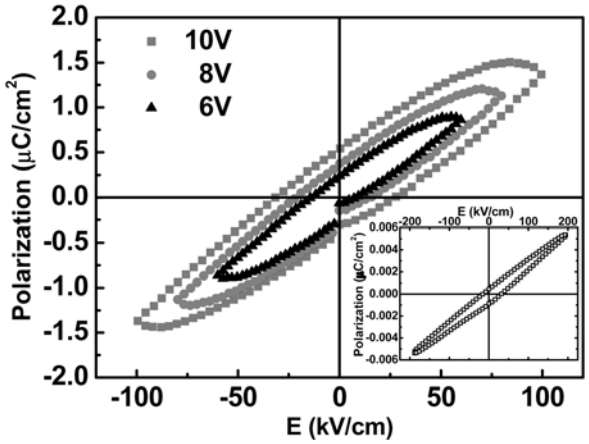

FIG. 4. (Color online) P-E hysteresis loops of BNT nanotube arrays with parallel AAO template. Inset is the P-E loop of pure AAO templates.

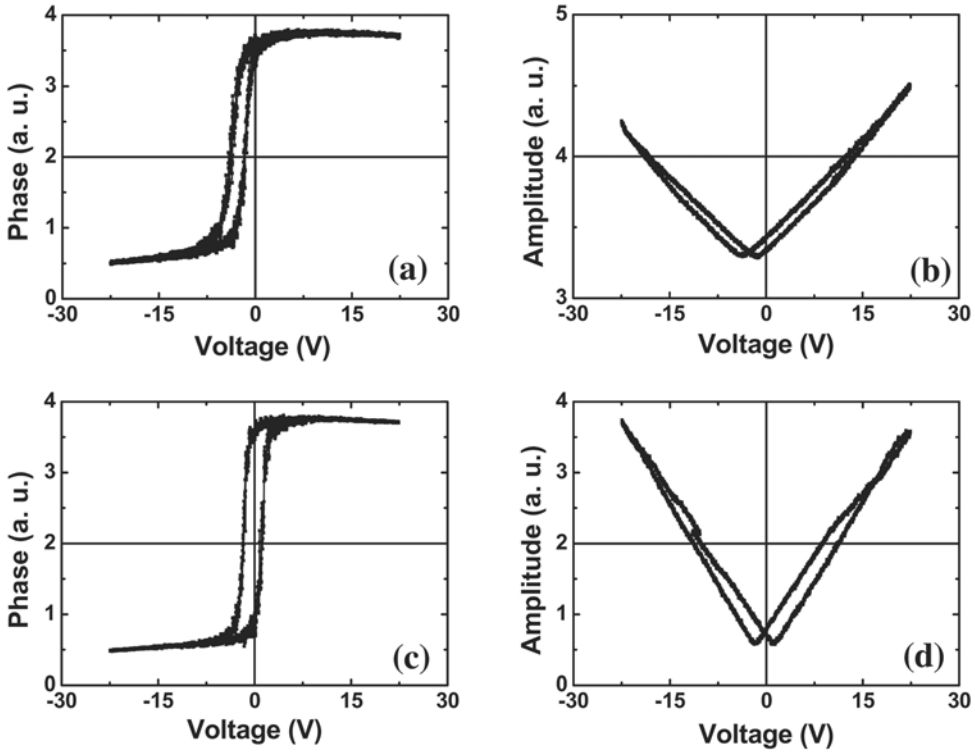

FIG. 5. Out-of-plane piezoresponse (a) phase and (b) amplitude loops, and in-plane piezoresponse (c) phase and (d) amplitude loops of individual BNT nanotubes measured by PFM.

Retention property of ferroelectrics also plays an important role in the reliability and lifetime of FeRAM. Figure 6 shows the retention property of the BNT nanotube. It can be seen that the BNT nanotube completely switches after applying a dc bias of 40 V on the scanned region [Figs. 6(b) and 6(c)]. The polarization state of the nanotube remains after 10^5 s [Fig. 6(d)]. It was reported that PZT nanodots could be individually addressed and showed promising switchable and retention properties under PFM.[33]

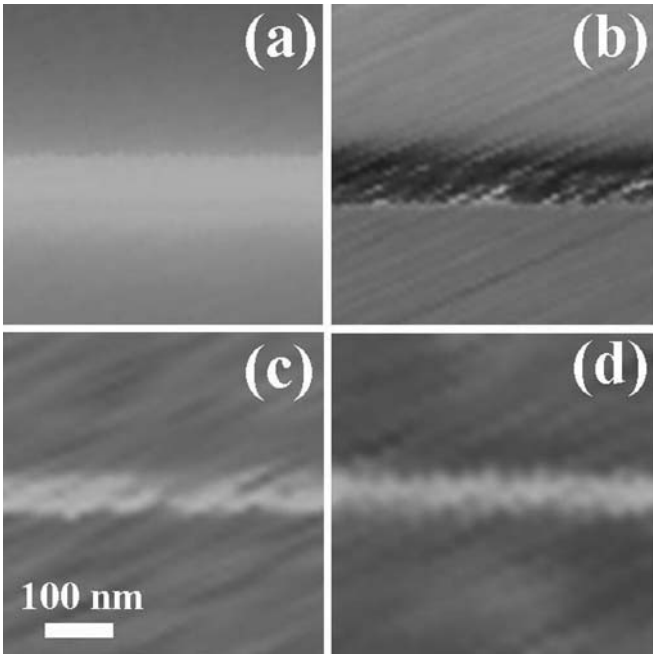

FIG. 6. (Color online) (a) Topography image of BNT nanotube, and out-of-plane piezoresponse phase image (b) before, (c) right after, and (d) 10^5 s after 40 V dc polar scan.

IV. CONCLUSION

In summary, BNT nanotubes with outer diameter of about 100 nm, wall thickness of about 30 nm, and length of about 50 μm were fabricated using a sol-gel process with AAO templates. The remnant polarization and dielectric constant of BNT nanotube arrays in an AAO template are comparable to those of BNT thin films. Well-defined piezoresponse phase and amplitude loops of individual BNT nanotubes are obtained by PFM in both out-of-plane and in-plane directions, and the loops are asymmetric. The nanotube is switchable in the transverse direction and shows long term retention. All results indicate that the BNT nanotubes could have potential applications in lead-free electronic microstructures and 3D stacking of non-volatile ferroelectric memories.

ACKNOWLEDGMENTS

This work was supported by the National Science Foundation (No. 50972056 and 51002075) and the 973 Project of MOST (2009CB623303 and 2009CB929501). One of the authors Y. Kan wishes to thank China Postdoctoral Science Foundation (Nos. 20090461077 and 201003574) and Jiangsu Provincial Postdoctoral Foundation (No. 0902001B).

[1]M. Dawber, K. M. Rabe, and J. F. Scott, Rev. Mod. Phys. **77**, 1083 (2005).
[2]N. Setter, D. Damjanovic, L. Eng, G. Fox, S. Gevorgian, S. Hong, A. Kingon, H. Kohlstedt, N. Y. Park, G. B. Stephenson, I. Stolitch, A. K. Taganstev, D. V. Taylor, T. Yamada, and S. Streiffer, J. Appl. Phys. **100**, 051606 (2006).
[3]A. Gruverman and A. Kholkin, Rep. Prog. Phys. **69**, 2443 (2006).

[4]N. A. Pertsev, A. Petraru, H. Kohlstedt, R. Waser, I. K. Bdikin, D. Kiselev, and A. L. Kholkin, Nanotechnology **19**, 375703 (2008).
[5]D. A. Bonnell, S. V. Kalinin, A. L. Kholkin, and A. Gruverman, MRS Bull. **34**, 648 (2009).
[6]S. V. Kalinin, A. Rar, and S. Jesse, IEEE Trans. Ultrason. Ferroelectr. Freq. Control **53**, 2226 (2006).
[7]P. Paruch, T. Giamarchi, and J. M. Triscone, Phys. Rev. Lett. **94**, 197601 (2005).
[8]G. Catalan, H. Bea, S. Fusil, M. Bibes, P. Paruch, A. Barthelemy, and J. F. Scott, Phys. Rev. Lett. **100**, 027602(2008).
[9]V. V. Shvartsman, N. A. Pertsev, J. M. Herrero, C. Zaldo, and A. Kholkin, J. Appl. Phys. **97**, 104105 (2005).
[10]S. Jesse, B. J. Rodriguez, S. Choudhury, A. P. Baddorf, I. Vrejoiu, D. Hesse, M. Alexe, E. A. Eliseev, A. N. Morozovska, J. Zhang, L. Q. Chen, and S. V. Kalinin, Nature Mater. **7**, 209 (2008).
[11]T. Jungk, A. Hoffmann, and E. Soergel, Appl. Phys. Lett. **89**, 163507 (2006).
[12]A. Gruverman and S. V. Kalinin, J. Mater. Sci. **41**, 107 (2006).
[13]X. Y. Li, K. Kitamura, and K. Terabe, Appl. Phys. Lett. **89**, 132905 (2006).
[14]J. Junquera and P. Ghosez, Nature **422**, 6931 (2003).
[15]M. Abplanalp, J. Fousek, and P. Gunter, Phys. Rev. Lett. **86**, 5799 (2001).
[16]J. F. Scott, H. J. Fan, S. Kawasaki, J. Banys, M. Ivanov, J. Macutkevic, R. Blinc, V. V. Laguta, P. Cevc, J. S. Liu, and A. Kholkin, Nano Lett. **8**, 4404 (2008).
[17]S. S. Nonenmann, O. D. Leaffer, E. M. Gallo, M. T. Coster, and J. E. Spanier, Nano Lett. **10**, 542 (2010).
[18]Y. Luo, I. Szafraniak, N. D. Zakharov, V. Nagarajan, M. Steinhart, R. B. Wehrspohn, J. H. Wendorff, R. Ramesh, and M. Alexe, Appl. Phys. Lett. **83**, 440 (2003).
[19]S. S. N. Bharadwaja, M. Olszta, S. Trolier-McKinstry, X. Li, T. S. Mayer, and F. Roozeboom, J. Am. Ceram. Soc. **89**, 2695 (2006).
[20]J. Kim, S. A. Yang, Y. C. Choi, J. K. Han, K. O. Jeong, Y. J. Yun, D. J. Kim, S. M. Yang, D. Yoon, H. Cheong, K. Chang, T. W. Noh, and S. D. Bu, Nano Lett. **8**, 1813 (2008).
[21]X. Y. Zhang, C. W. Lai, X. Zhao, D. Y. Wang, and J. Y. Dai, Appl. Phys. Lett. **87**, 143102 (2005).
[22]W. Liu, X. H. Sun, H. W. Han, M. Y. Li, and X. Z. Zhao, Appl. Phys. Lett. **89**, 163122 (2006).
[23]F. D. Morrison, L. Ramsay, and J. F. Scott, J. Phys.: Condens. Matter **15**, L527 (2003).
[24]B. I. Seo, U. A. Shaislamov, S. J. Lee, S. W. Kim, I. S. Kim, S. K. Hong, and B. Yang, J. Cryst. Growth, **292**, 315 (2006).
[25]F. Wang, J. B. Wang, X. L. Zhong, B. Li, and Y. C. Zhou, J. Cryst. Growth, **311**, 4495 (2009).
[26]W. Cai, X. M. Lu, D. Li, H. F. Bo, R. W. Peng, X. B. Wu, Y. F. Liu, and J. S. Zhu, Appl. Phys. Lett. **94**, 092906 (2009).
[27]P. G. Graves, G. Hua, S. Myhra, J. G. Thompson, J. Solid State Chem., **114**, 112 (1995).
[28]R. Zallen, M. Slade, and A. T. Ward, Phys. Rev. B **3**, 4257 (1971).
[29]H. Idink, V. Srikanth, W. B. White, and E. C. Subbarao, J. Appl. Phys., **76**, 1819 (1994).
[30]A. N. Morozovska, E. A. Eliseev, and M. D. Glinchuk, Phys. Rev. B **73**, 214106 (2006).
[31]W. Li, J. Ma, C. H. Song, P. Bao, X. M. Lu, J. S. Zhu, Y. N. Wang, Chin. Phys. Lett. **21**, 544 (2004).
[32]A. K. Jonscher, *Dielectric Relaxation in Solids* (Chelsea Dielectric Press, London, 1983).
[33]W. Lee, H. Han, A. Lotnyk, M. A. Schubert, S. Senz, M. Alexe, D. Hesse, S. Baik, and U. Gosele, Nature Nanotechnol., **3**, 402 (2008).
[34]L. M. Eng, H. J. Guntherodt, G. A. Schneider, U. Kopke, and J. M. Saldana, Appl. Phys. Lett. **74**, 233 (1998).
[35]G. Suyal, E. Colla, R. Gysel, M. Cantoni, and N. Setter, Nano Lett. **4**, 1339 (2004).
[36]C. Harnagea, A. Pignolet, M. Alexe, D. Hesse, and U. Gosele, Appl. Phys. A **70**, 261 (2000).
[37]Z. Y. Wang, J. Hu, and M. F. Yu, Appl. Phys. Lett. **89**, 263119 (2006).
[38]S. Hong, J. Woo, H. Shin, J. U. Jeon, Y. E. Pak, E. L. Colla, N. Setter, E. Kim, and K. No, J. Appl. Phys., **89**, 1377 (2001).
[39]A. Roelofs, U. Bottgre, R. Waser, F. Schlaphof, S. Trogisch, and L. M. Eng, Appl. Phys. Lett. **77**, 3444 (2000).